Numerical Analysis of Pylon-Blowing Systems for Pusher-Propeller Applications

Jindal, Aman; Sinnige, Tomas; Hulshoff, Steven; Veldhuis, Leo

DOI
10.2514/6.2017-3908

Publication date
2017

Document Version
Accepted author manuscript

Published in
35th AIAA Applied Aerodynamics Conference

This is an Accepted Manuscript of an article published in: 35th AIAA Applied Aerodynamics Conference 5-9 June 2017, Denver, Colorado. ISBN: 978-1-62410-501-2
Available online: https://arc.aiaa.org/doi/10.2514/6.2017-3908

Numerical Analysis of Pylon-Blowing Systems for Pusher-Propeller Applications

Aman Jindal*, Tomas Sinnige†, Steven J. Hulshoff‡, and Leo L. M. Veldhuis§
Delft University of Technology, Delft, 2629 HS, the Netherlands

Pylon-blowing systems provide an effective way of minimizing the interaction effects due to pylon-wake impingement experienced by pusher propellers. This paper presents a numerical study of the uniformity of the blown pylon wake as a function of blowing-slot geometry and blowing momentum coefficient. The flow around the pylon was simulated by solving the steady-state Reynolds-averaged Navier–Stokes equations. The numerical setup was validated using experimental data for both trailing-edge blowing and chordwise blowing configurations. If experimental error is neglected, the model error for the chordwise blowing layout was 15–17%. It was shown that maximal wake uniformity was achieved for a chordwise blowing configuration with the blowing slots positioned at $x/c = 0.7$. This location provided the best compromise between boundary-layer thickness upstream of the blowing slot, available mixing length, and boundary-layer development downstream of the slot. The corresponding optimal blowing coefficient resulted in a slight velocity overshoot in the boundary layer at the pylon trailing edge. This overshoot then mixed with the deficit associated with the boundary layer formed downstream of the blowing slot to arrive at a nearly uniform velocity profile in the pylon wake. Under asymmetric inflow conditions, the chordwise blowing approach provided effective wake filling if the blowing coefficients on upper and lower surfaces were separately matched with the local boundary-layer thickness at the blowing slot. A linear relation between required blowing rate and boundary-layer thickness was found. Following this approach, the resulting wake was made nearly uniform at an angle of attack of 9°.

I. Introduction

THE high propulsive efficiency of propeller propulsion systems offers significant economic and environmental benefits over current-generation turbofan engines. However, the integration of advanced propellers with the airframe poses difficulties in terms of ground clearance and cabin noise. A configuration study by Page et al.[1] showed that a pylon-mounted pusher configuration offers the best compromise between aerodynamic and aeroacoustic performance. Yet, in such a layout the propeller operates in the wake of the upstream pylon. As a result, the blades periodically experience a reduction in inflow velocity, causing an unsteady angle-of-attack perturbation. This leads to unsteady blade loads and an associated noise penalty, as confirmed in the literature for both single-rotating[2,3] and contra-rotating[4–7] propeller configurations.

The velocity deficit in the pylon wake governs the pylon–propeller interaction phenomena. Therefore, pylon-wake control can be applied to mitigate the pylon-installation effects. Among the possible flow-control strategies, the active technique of pylon blowing has shown to successfully eliminate the noise penalty due to the wake-impingement effects in various experimental[4–6,8,9] and numerical[7,10] studies. The work by Sinnige et al.[9] confirmed that the achieved noise reductions are due to the abatement of the unsteady blade-load fluctuations, which is a direct result of the improved uniformity of the propeller inflow with blowing enabled.

Pylon-blowing systems can be grouped into two categories: trailing-edge blowing and chordwise blowing configurations. The trailing-edge blowing system consists of a single outlet in the pylon trailing edge, whereas

*M.Sc. Student, Aerodynamics Section, Faculty of Aerospace Engineering.
†Ph.D. Candidate, Flight Performance and Propulsion Section, Faculty of Aerospace Engineering, T.Sinnige@tudelft.nl; AIAA member.
‡Assistant Professor, Aerodynamics Section, Faculty of Aerospace Engineering.
§Full Professor, Head of Flight Performance and Propulsion Section, Faculty of Aerospace Engineering, AIAA Member.

the chordwise approach involves a blowing slot positioned along the chord on both sides of the pylon. In terms of the uniformity of the pylon wake, the chordwise blowing system offers superior performance compared to the trailing-edge blowing variant.[11] For the latter, the short mixing length available between the trailing edge of the pylon and the propeller causes wake profiles characterized by a velocity overshoot on the wake centerline with velocity deficits on both sides.[9] The chordwise blowing approach, on the other hand, provides increased mixing length, and thinner boundary layers at the positions of the blowing slots. Experiments have shown that a high degree of uniformity of the pylon wake can be achieved using the chordwise blowing approach.[8] Recent work by Bury et al.[12] successfully attempted to further improve upon the uniformity of the blown pylon wake by combining chordwise blowing with an upstream boundary-layer scooping system. In this way, the pylon wake was made even more uniform, at the cost of additional complexity.

Previous work has confirmed the potential for significant improvements of the uniformity of the downstream wake using pylon blowing. However, so far no consideration has been given to the optimal layout of the blowing system in terms of the positioning of the blowing slots. Also, the performance of pylon blowing has only been evaluated under symmetric inflow conditions, whereas in a more realistic scenario the pylon–propeller combination might also operate at an angle of incidence to the incoming flow. The numerical study presented in the current paper aimed at filling these gaps. By comparing the downstream wake uniformity for a range of blowing slot parameters, increased understanding is obtained of the sensitivity of the pylon wake to the design of the blowing system. Moreover, the robustness of the blowing system under asymmetric inflow conditions is discussed, and an approach is presented to estimate the required blowing rates for the asymmetric case based on reference values obtained for symmetric inflow.

II. Pylon Chordwise Blowing

The goal of the pylon-blowing system is to minimize the velocity deficit in the pylon wake upstream of the propeller. The blowing slots can be integrated into the trailing edge or along the chord of the pylon. This paper focuses on the chordwise blowing solution, while the trailing-edge blowing layout is considered for comparison purposes only. In a chordwise blowing system, a slot is positioned on both surfaces of the pylon, tangentially blowing high-speed jets to re-energize the boundary layer that develops on the pylon surface. The typical layout of such a chordwise blowing system is illustrated in Fig. 1.

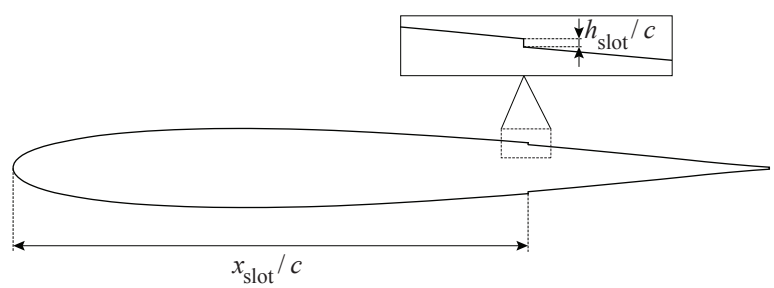

Figure 1. Typical layout of an airfoil with chordwise blowing system.

To minimize the nonuniformity in the pylon wake, the high-momentum blowing jets are mixed with the boundary-layer flow on the pylon surface. This is illustrated in Fig. 2, which represents a generic shape of the velocity profile of the boundary layer with blowing enabled. The blown velocity profile is characterized by two parameters: a velocity deficit δ_d and a velocity overshoot δ_{os}. The velocity deficit represents the remainder of the momentum loss due to the upstream boundary layer, while the overshoot is due to the injection of the high-speed blowing jet. This velocity overshoot is the driving factor in compensating for the velocity deficit that develops on the pylon surface downstream of the blowing slot. This is treated in more detail in the discussion of the results.

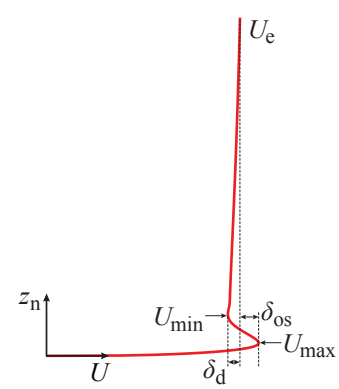

Figure 2. Typical boundary-layer profile downstream of chordwise blowing slot.

A typical chordwise blowing system can be characterized by three top-level design parameters:

1. **Chordwise location of the blowing slots:** the axial position of the slots x_{slot}/c drives the uniformity of the blown wake. By moving the slots upstream, the mixing length can be increased, at the cost of additional momentum deficit generated downstream of the slots.

2. **Slot height:** the slot height h_{slot}/c was considered as the most important geometrical characteristic of the blowing slot itself. At a given outflow momentum, the slot height affects the velocity of the blown jets.

3. **Slot blowing coefficient:** the slot blowing coefficient C_μ is a measure of the momentum of the air blown into the pylon wake. For an incompressible flow with equal densities of the freestream and blown air, C_μ is defined as:

$$C_\mu = 2\frac{h_{\text{slot}}}{c}\frac{U_{\text{j}}^2}{U_\infty^2}, \tag{1}$$

with c the pylon chord, h_{slot} the slot height, U_{j} the velocity of the blown jet, and U_∞ the freestream velocity.

Depending on the selected combination of design parameters, the velocity profile in the blown wake will have different characteristics. Five generic types of velocity profiles can be identified, as shown in Fig. 3.

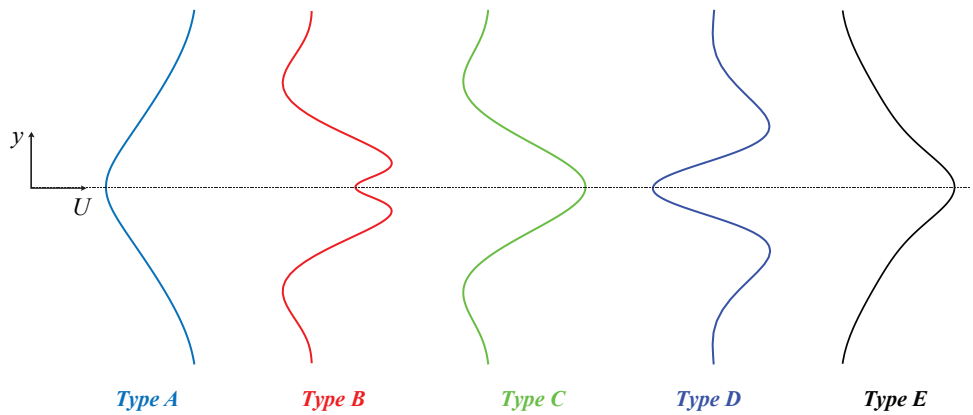

Figure 3. Overview of the different types of velocity profiles in the pylon wake.

- **Type A:** this velocity profile is characteristic of the unblown pylon, and is also obtained at very small blowing momentum coefficients.

- **Type B:** increasing the blowing rate, the blown jets start to re-energize the pylon boundary layer. Two velocity overshoots appear around the wake center because of the high-momentum blowing jets. The central velocity deficit is due to the momentum deficit in the boundary layers developing downstream of the blowing slots. Additionally, two minima occur near the wake edges due to insufficient mixing between the boundary layer upstream of the blowing slot and the blown jets.

- **Type C:** by further increasing the blowing rate, the central velocity deficit is eliminated because of enhanced mixing with the blown jets. The remaining minima near the wake edges indicate that a longer mixing length is required to accelerate the boundary layers developed upstream of the blowing slot. This type of velocity profile is also typical for trailing-edge blowing configurations.

- **Type D:** an increased mixing length can be provided by moving the chordwise blowing slots upstream. In this way, the velocity minima near the wake edges can be eliminated. However, the increased distance from the blowing slot to the trailing edge introduces an increased deficit on the wake centerline if the blowing rate is insufficiently high.

- **Type E:** increasing the blowing rate compared to the type-D profile, the central velocity deficit is turned into a velocity overshoot.

The response of the propeller with the pylon installed is a function of both the integral velocity deficit and the maximum velocity gradients in the wake. To quantify the uniformity of the blown pylon wake, an integral criterion was therefore defined that includes both the total area of the velocity deficit as well as the difference between maximum and minimum axial velocity in the wake. The resulting parameter is referred to as the W-criterion in the following, and is defined as:

$$W = A\left(\frac{U_{\max} - U_{\min}}{U_{\mathrm{e}}}\right), \tag{2}$$

with $U_{\max}$ and $U_{\min}$ the maximum and minimum velocities in the pylon wake, U_{e} the local undisturbed velocity, and the integral wake velocity deficit A defined as:

$$A = \int_{-b_{\mathrm{w}}/c}^{+b_{\mathrm{w}}/c} \left|1 - \frac{U}{U_e}\right| \mathrm{d}\frac{Y}{c}, \tag{3}$$

with b_{w}/c the normalized semiwidth of the wake and Y/c the normalized lateral coordinate through the wake. The semiwidth of the wake was defined as the distance between the wake center and the lateral position at which the axial velocity had recovered to 99% of the local undisturbed axial velocity (U_{e}).

III. Numerical Setup

A numerical investigation was performed of the flow around a two-dimensional pylon profile with chordwise blowing system. The goal was to find an optimized design for mitigating the velocity deficit in the downstream wake. Before this optimization study was started, the numerical setup was validated using experimental data for the unblown and blown cases, involving both trailing-edge blowing and chordwise blowing configurations.

A. Geometry

A symmetric NACA0010 airfoil was chosen as the starting point and was then modified to incorporate chordwise blowing slots on both upper and lower surfaces, as shown before in Fig. 1. The blowing slots were introduced by an inward displacement of the profile downstream of the blowing slot. The magnitude of the vertical shift was based on the selected blowing-slot height, which is also one of the parameters considered in the design optimization study. The selected airfoil had a chord length of 1 m and was simulated for a freestream velocity of 30 m/s, obtaining a chordwise Reynolds number of $1.9 \cdot 10^6$.

The validation studies were performed for different geometries and operating conditions, imposed by those considered in the experiments from which data were available. The details are discussed for the trailing-edge blowing and chordwise blowing configurations separately in Subsection III.C.

B. Modeling

The flow around the pylon was simulated by solving the Reynolds-averaged Navier–Stokes equations using a commercial finite-volume solver. Steady-state simulations were performed, in which the pylon boundary layer was considered as fully turbulent. Various turbulence models were tested for their predictive capability for the case of the pylon-wake flow, using experimental data measured by Nakayama[13]. The numerical data computed using the various turbulence models were compared to the experimental results in terms of the wake width, wake area, and maximum deficit in the wake at $x/c = 1.01$. The Spalart–Allmaras turbulence model resulted in the smallest offset from the experimental data by Nakayama, and was therefore selected for all subsequent computations.

The solutions were obtained using a pressure-based solver with a segregated algorithm. The interpolation procedures for momentum and eddy viscosity were carried out using a second-order upwind scheme, while a least-squares cell-based approach was used to calculate the gradients of scalar variables. The coupling of pressure and velocity was done using the SIMPLEC (Semi-Implicit Method for Pressure-Linked Equations-Consistent) algorithm, while the pressure interpolation was performed using a second-order scheme. The solution was initialized from the inlet boundary condition in order to start the iterative process used to reach a converged solution. Convergence of the numerical solution was monitored using the integral of the velocity magnitude in the pylon wake.

The flow domain and the respective boundary conditions used for the simulations are shown in Fig. 4. Pressure inlet and pressure outlet boundary conditions were prescribed on the inlet and outlet boundaries. For symmetric inflow conditions ($\alpha = 0°$), the upper and lower walls were treated as slip walls and were verified to be sufficiently far away from the airfoil to model the velocity perturbations on them as zero. In case of asymmetric inflow ($\alpha \neq 0°$), the upper and lower boundaries were treated as pressure inlets and pressure outlets, depending on the direction of the asymmetry. The airfoil model was treated as solid wall, while the outflow from the blowing slots was specified using velocity inlet boundary conditions.

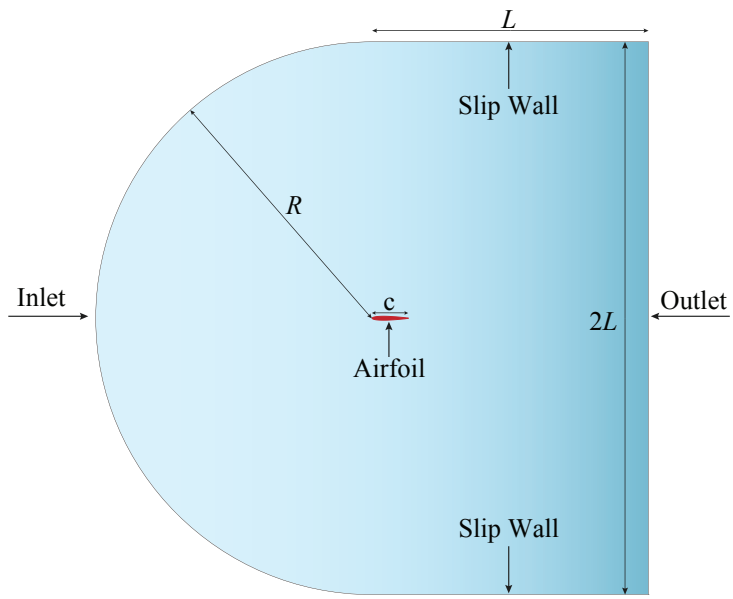

Figure 4. Flow domain and boundary conditions for the simulations with symmetric inflow conditions.

Five domains (see Fig. 4) of increasing size, $R/c = L/c = [20, 40, 100, 200, 500]$, were tested on a baseline airfoil case without blowing to select the smallest domain for which the solution was found to be independent of the domain size. This was assessed by extracting velocity profiles in the pylon wake at $x/c = 1.01$, and investigating the wake width, area, and maximum deficit for the five domain sizes. The corresponding results are depicted in Fig. 5, in which the data are normalized with the values obtained for the largest domain.

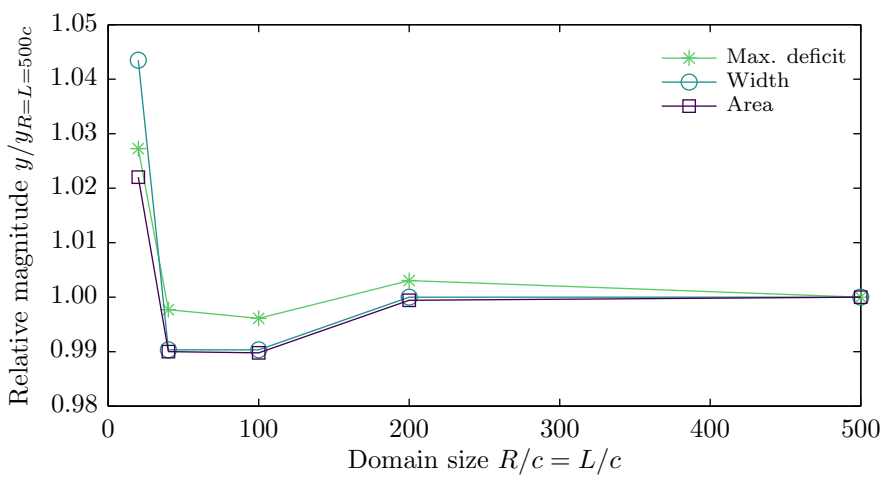

Figure 5. Results of the domain-independence test.

Figure 5 shows that from a domain size of $R/c = L/c = 40$ onward, the results were within approximately 1% of the data computed with the largest domain. Therefore, this domain size was considered adequate and was selected for all subsequent simulations.

A structured multiblock C-mesh was generated for the domain around the airfoil. Refinements were applied to capture the flow physics downstream of the blowing slots and in the wake region. The normal spacing at the first cell adjacent to the airfoil surface was chosen to lie inside the viscous sublayer ($y^+ \leq 1$) of the developed boundary layer. Appropriate regions of refinement were determined from the results of the mesh-convergence study described in Section C. The final mesh used for the chordwise blowing layout featured a y^+ value of 0.25 and consisted of about $3.5 \cdot 10^5$ quadrilateral elements. It is shown in Fig. 6.

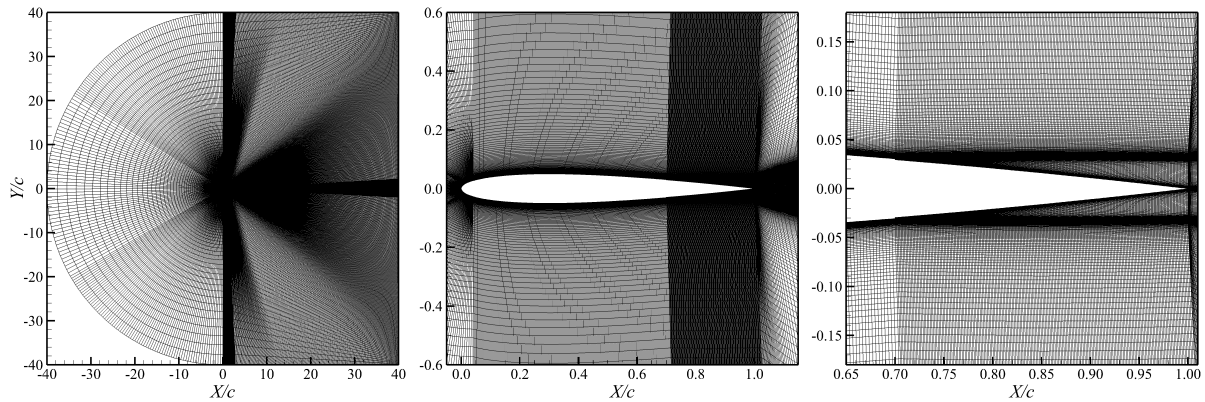

Figure 6. Visualization of the final mesh used for the simulations of the chordwise blowing layout.

C. Error Estimation

The numerical setup was validated for both trailing-edge and chordwise blowing configurations using experimental data as reference. For both cases, three meshes were considered, referred to as fine, medium, and coarse, related by a mesh-refinement factor of 2. For the chordwise blowing case, Richardson extrapolation[14,15] and Roache's grid convergence index (GCI)[16,17] were used to perform a systematic mesh-refinement study and quantify the discretization errors.

1. Trailing-Edge Blowing

The performance of the numerical setup for the pylon trailing-edge blowing configuration was assessed by comparison with experimental data measured at Delft University of Technology's Low-Turbulence Tunnel. This closed-section, closed-return wind tunnel features a maximum wind speed of 120 m/s in the octagonal test section of $1.80 \times 1.25 \times 2.60$ m. Owing to the large contraction ratio of 17.8, the tunnel provides a low turbulence level of less than 0.1%. The pylon geometry and pylon-blowing system discussed in Ref. 9 were used. The pylon featured a straight, untapered planform with a chord length of 0.489 m and a cross-section defined by a modified NACA 0010 profile. The pylon model was mounted on the floor of the test section, with a free tip at the other end. For the symmetric inflow case considered here, the wake characteristics at the measurement location were verified to be unaffected by three-dimensional effects. A photograph of the pylon model installed in the wind tunnel is shown in Fig. 7.

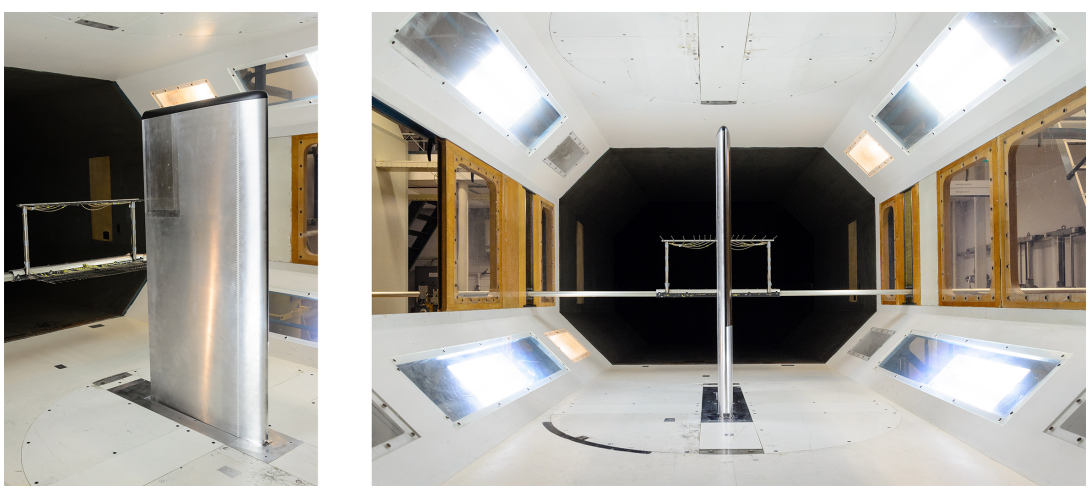

Figure 7. Pylon model and downstream wake rake installed in the wind tunnel.

The total and static pressures in the wake of the pylon were measured using a wake rake positioned at $0.3c$ downstream of the pylon trailing edge, as also shown in Fig. 7. An electronic pressure scanner was used to record all pressures simultaneously at a given vertical position in the wake. The measurements were taken at a freestream velocity of 60 m/s. A range of blowing rates was considered to study the sensitivity of the pylon-wake profiles to the blown mass flow. The blowing rate was controlled by changing the inlet pressure to the blowing system, and was monitored using a VPInstruments VPF-R200-M100 flow meter. The experimental data considered in this paper were acquired under symmetric inflow conditions ($\alpha = 0°$).

Three blowing rates were selected for the simulations, for which in this case a first-order upwind scheme was used for the discretization of the eddy viscosity. Figure 8 compares simulation and experiment in terms of distributions of the total-pressure ratio in the wake. The coarse, medium, and fine meshes were found to have minimum values of wall-normal distance y^+ of 0.2500, 0.1250, and 0.0625, respectively.

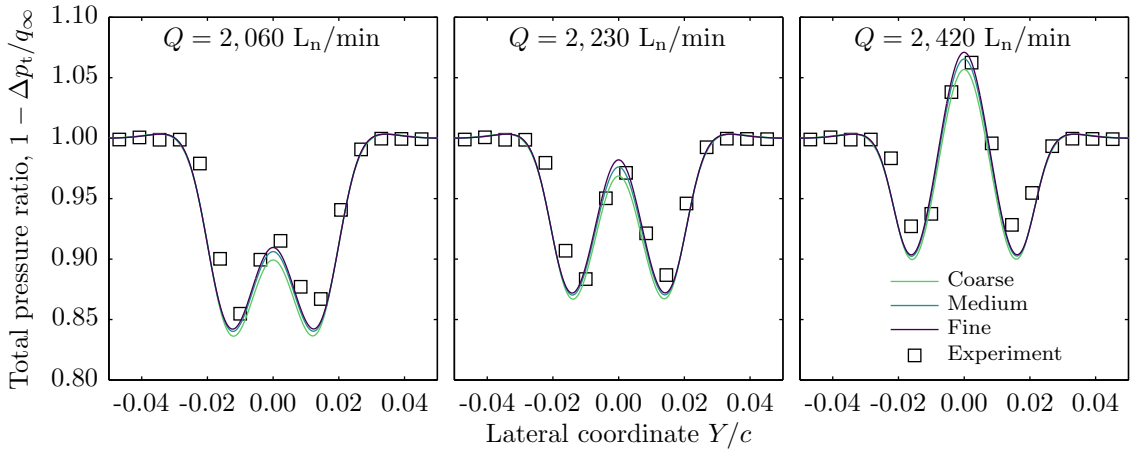

Figure 8. Computed and measured distributions of the total pressure in the wake of the pylon with trailing-edge blowing; $x/c = 1.3$.

Figure 8 shows good agreement between the numerical and experimental data for the three blowing rates considered. The simulations returned a representative prediction of the shape of the total pressure profile, while also the local maximum on the wake centerline followed the expected trend. The deficit at the two local minima in the wake, on the other hand, seemed overpredicted in the simulations. However, this could also be due to the limited spatial resolution of the experimental data.

Comparing the numerical results for the different meshes, it is observed that the medium and fine meshes show practically equivalent results. The convergence of the numerical data was quantified using the integrated squares of the total pressure change in the wake as integral parameter:

$$A_{p_t} = \int_{-b_w/c}^{+b_w/c} \left(1 - \frac{\Delta p_t}{q_\infty}\right)^2 \mathrm{d}\frac{Y}{c}. \tag{4}$$

The values computed using Eq. (4) are reported in Table 1.

Table 1. Numerical values of the integrated total pressure deficit A_{p_t} for the trailing-edge blowing case; $x/c = 1.3$.

Q [L$_n$/min]	$A_{p_t}^{\text{coarse}}$	$A_{p_t}^{\text{medium}}$	$A_{p_t}^{\text{fine}}$
2,060	$7.67 \cdot 10^{-4}$	$7.23 \cdot 10^{-4}$	$7.02 \cdot 10^{-4}$
2,230	$4.15 \cdot 10^{-4}$	$3.86 \cdot 10^{-4}$	$3.71 \cdot 10^{-4}$
2,420	$2.06 \cdot 10^{-4}$	$2.02 \cdot 10^{-4}$	$2.03 \cdot 10^{-4}$

Table 1 indicates that the integral wake deficit defined by Eq. (4) displayed monotonic convergence at the two lowest blowing rates. The corresponding order of convergence was equal to 1.0 at $Q = 2,060$ L$_n$/min and 0.9 at $Q = 2,230$ L$_n$/min. A nonmonotonic behavior was observed at the highest blowing rate. This was because the total-pressure maximum on the wake centerline showed a different convergence rate than the surrounding local minima. Based on these results, it is concluded that the discretization was not in the asymptotic region, hence a formal error estimation could not be performed for the trailing-edge blowing case.

2. Chordwise Blowing

Experiments performed by Pfingsten[18] using the DLR-F15 geometry[19,20] were taken as the validation case for the chordwise blowing configuration. In this study, a modern transonic profile was used to investigate circulation control using steady blowing jets over a Coanda surface. The chord length of the model equaled $c = 0.3$ m, with a Reynolds number referenced to the chord of $Re_c = 1 \cdot 10^6$. The blowing slot was placed directly upstream of a high-lift flap positioned at $x/c = 0.7$, with a flap deflection angle of $\delta_f = 40°$. The height of the slot was $h_{slot}/c = 0.0001$. The experiments were conducted at a freestream velocity of $U_\infty = 50$ m/s, resulting in a Mach number of $M = 0.15$. The aerodynamic performance of the airfoil was analyzed for different blowing momentum coefficients C_μ.

Numerical simulations were performed for the experimental geometry and flow conditions. Again three meshes were used, in this case with minimum values of nondimensional wall distance y^+ of 0.500, 0.250, and 0.125 for the coarse, medium, and fine meshes, respectively. The resulting velocity profiles were extracted downstream of the blowing slot at $x/c = 0.715$ and compared with the measured data. Two different blowing momentum coefficients were considered, corresponding to $C_\mu = [0.033, 0.040]$. The numerical and experimental data were compared in terms of the integral of the absolute velocity deficit in the boundary layer. This scalar value was defined similarly to Eq. (3), but then with integration limits from zero to the edge of the boundary layer. Table 2 compares the results for the numerical and experimental data. The corresponding error estimation is provided in Table 3.

Table 2. Ratio between numerical and experimental deficit area in the boundary layer of the pylon with chordwise blowing; $x/c = 0.715$. Experimental data taken from Ref. 18.

C_μ	$\frac{A_c}{A_{exp}}$	$\frac{A_m}{A_{exp}}$	$\frac{A_f}{A_{exp}}$
0.033	1.195	1.177	1.173
0.040	1.188	1.161	1.157

Table 3. Error estimation for the chordwise blowing configuration.

C_μ	P [-]	ϵ_{disc} [%]	GCI [%]	f_{exact} [-]	ϵ_{model} [%]
0.033	2.41	0.5	1.5	0.133	17.1
0.040	2.37	0.5	1.6	0.145	15.6

Tables 2 and 3 show that the discretization error ϵ_{disc} is much smaller than the model error ϵ_{model}, indicating almost no dependency of the numerical solution on the mesh size. The model error was highest at the low blowing momentum case, at which an error of 17.1% was obtained. Based on the observed mesh convergence, the medium mesh was considered as an appropriate choice to carry out further simulations. Therefore, all results presented in the remainder of this paper for the chordwise blowing layout were obtained using the medium mesh ($y^+ = 0.25$).

IV. Results

A. Chordwise Pylon-Blowing System Design

The pusher-propeller installation effects are caused by the velocity perturbations in the pylon wake impinging on the propeller blades. A flow-control system using chordwise blowing was therefore designed to minimize this velocity deficit in the propeller inflow. A blowing slot was positioned on both surfaces of the pylon, tangentially blowing high speed jets to re-energize the boundary layer that develops on the pylon surface.

1. Setup

The objective of the blowing-system design was to minimize the nonuniformity of the pylon wake, as quantified by the W-criterion defined by Eq. (2). The optimization was performed following an exhaustive-search approach, involving the three design variables discussed in Section II. The distinct levels considered for the design variables are listed in Table 4. Note that the values of the blowing coefficient are defined per slot.

Table 4. Considered values of the design variables.

x_{slot}/c	h_{slot}/c	C_μ
0.6	$5.0 \cdot 10^{-4}$	0.0009
0.7	$7.5 \cdot 10^{-4}$	0.0020
0.8	$1.0 \cdot 10^{-3}$	0.0036
0.9		0.0056
		0.0080
		0.0109
		0.0123
		0.0142

The optimization was performed assuming symmetric inflow. Table 5 provides a complete overview of the flow conditions considered in the design study.

Table 5. Flow conditions considered in the optimization study.

Parameter	Symbol	Value
Angle of attack	α	$0°$
Angle of sideslip	β	$0°$
Freestream velocity	U_∞	30 m/s
Atmospheric pressure	P	$101,325$ Pa
Density	ρ_∞	1.1835 kg/m^3
Temperature	T_∞	298 K
Reynolds number	Re_c	$1.9 \cdot 10^6$

The value of the W-criterion was extracted from all simulations along lines at three different axial positions in the pylon wake, as illustrated in Fig. 9. These positions were selected to span the typical range of pylon–propeller spacings observed for pusher-propeller configurations.

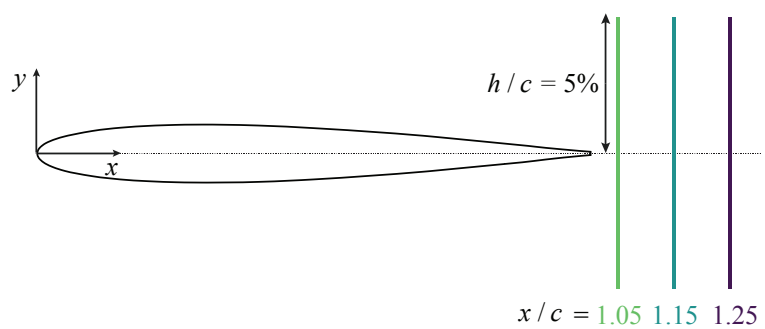

Figure 9. Illustration of the locations of the wake planes used in the design study.

2. Results

Simulations were performed for each combination of the values of the three design variables given in Table 4. Analysis of the results showed that the slot height had a comparatively small effect on the uniformity of the wake profiles. This was as expected, considering that it is also included in the definition of the blowing coefficient following Eq. (1). Therefore, initially the optimal chordwise slot location and blowing coefficient were determined with the slot height fixed at $h_{\text{slot}}/c = 1.0 \cdot 10^{-3}$. Figure 10 presents contours of the W-criterion as a function of chordwise slot location and blowing momentum coefficient, as extracted from the wake plane at $x/c = 1.25$.

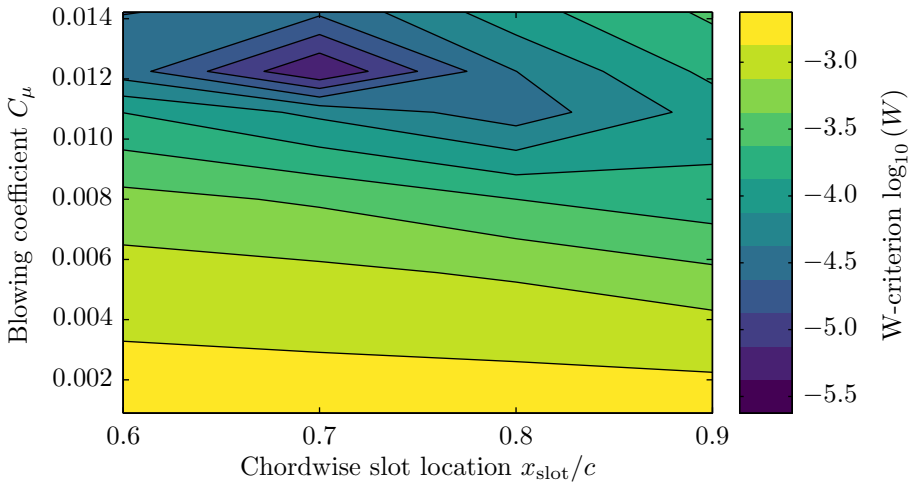

Figure 10. Wake uniformity versus chordwise slot location and blowing coefficient; $x/c = 1.25$, $h_{\text{slot}}/c = 1.0 \cdot 10^{-3}$.

It can be seen in Fig. 10 that optimal wake filling (minimum value of W) occurred for a slot located at $x_{\text{slot}}/c = 0.7$ and a blowing momentum coefficient of $C_\mu = 0.0123$. At lower blowing coefficients ($C_\mu \leq 0.010$), the blown jets were not sufficiently strong to overcome the momentum deficit of the boundary layer downstream of the slots, resulting in a type-D velocity profile. Therefore, for these cases the wake uniformity improved by moving the slot location toward the pylon trailing edge. At higher blowing settings, on the other hand, a downstream slot location provided insufficient mixing length for the blown jets to mix with the external flow and the wake profile to become uniform, leading to a type-B velocity profile. Therefore, the most favorable chordwise slot location was shifted upstream, until the optimum was reached at $x_{\text{slot}}/c = 0.7$ with a blowing momentum coefficient of $C_\mu = 0.0123$.

From Fig. 10 it can also be noted that for a fixed location of the blowing slot, the wake uniformity initially increases upon increasing C_μ but then starts to deteriorate again at higher blowing coefficients. At these settings, a strong overcompensation of the velocity deficit in the boundary layer occurs. This initially results in the type-C velocity profile shown in Fig. 3, which then develops into a type-E profile when the blowing rate is further increased.

To investigate the development of the pylon wake in the axial direction, the wake characteristics were also extracted at $x/c = 1.05$ and $x/c = 1.15$. This is important for the selection of the optimal pylon–propeller spacing for pusher-propeller configurations. Figure 11 presents the sensitivity of the wake uniformity to the axial position in the pylon wake. The optimal slot parameters and the resulting value of the W-criterion at the three axial positions are summarized in Table 6. Further optimization work with more sophisticated methods could refine the optima obtained with the exhaustive-search approach taken in this paper.

Table 6. Maximum wake uniformity versus axial distance from the pylon trailing edge; $h_{\text{slot}}/c = 1.0 \cdot 10^{-3}$.

x/c	x^*_{slot}/c	C^*_μ	$\log_{10}(W^*)$
1.05	0.8	0.0109	−3.95
1.15	0.7	0.0123	−4.77
1.25	0.7	0.0123	−5.70

Figure 11 and Table 6 show that the wake uniformity improves with increasing distance from the trailing edge of the pylon. This is as expected considering the associated increase in mixing length available for the blowing jets to mix with the freestream flow. Close to the pylon trailing edge, the sensitivity of the wake uniformity to the axial position is stronger than further downstream. This can be seen in Fig. 11 and Table 6 by noting that the decrease of the value of the W-criterion upon moving from location $x/c = 1.05$ to $x/c = 1.15$ is larger than when going from $x/c = 1.15$ to $x/c = 1.25$. At the most downstream wake plane considered ($x/c = 1.25$), a maximum improvement of the wake uniformity of 99.7% was achieved compared to the unblown result.

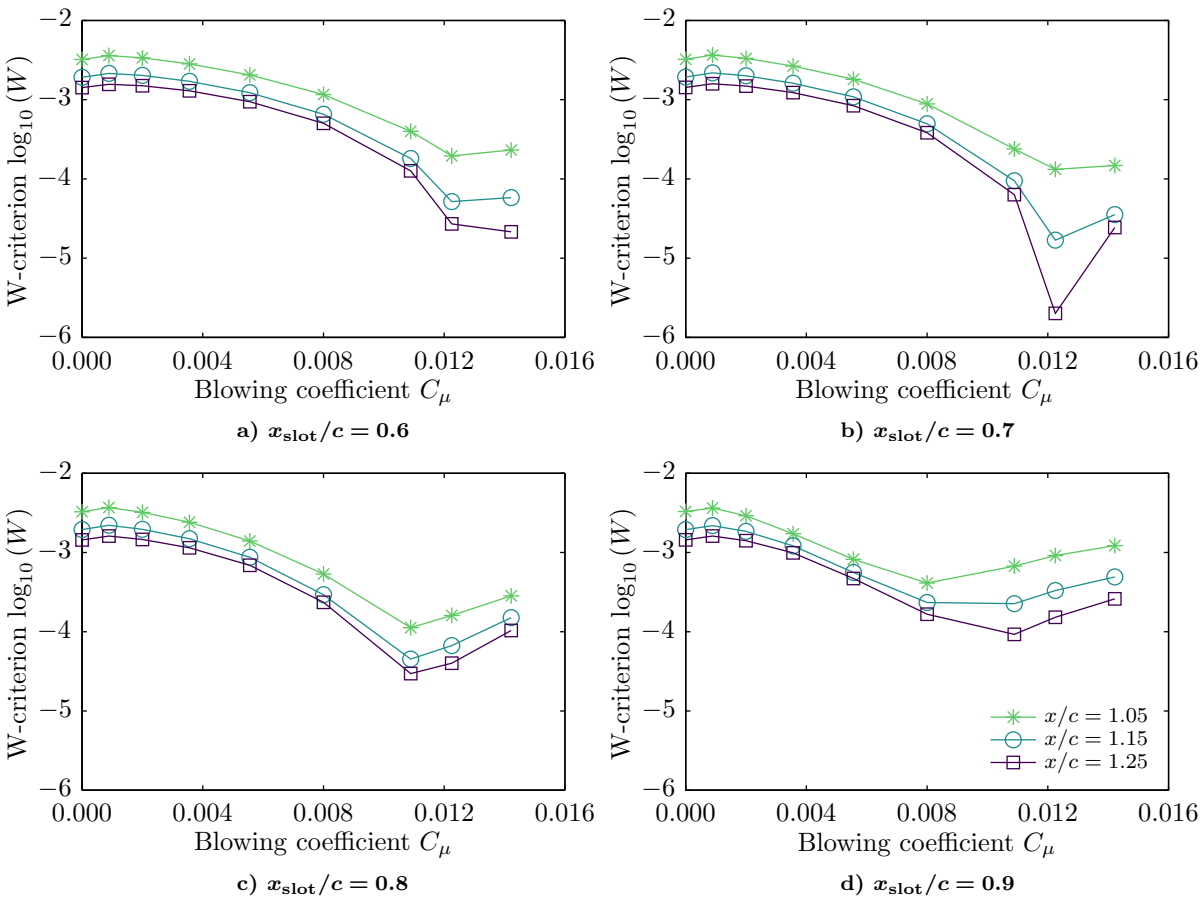

Figure 11. Sensitivity of wake uniformity to axial position in the pylon wake; $h_{\text{slot}}/c = 1.0 \cdot 10^{-3}$.

From Fig. 11 it can be concluded that the optimal blowing coefficient decreases upon moving the slot closer to the trailing edge of the pylon, at all axial evaluation planes considered. For slots located close to the trailing edge, the mixing length is relatively short, resulting in a type-B velocity profile (Fig. 3) with two pronounced overshoots in the velocity profile caused by the blowing jets. By reducing the blowing coefficient, these overshoots are minimized and thereby the wake uniformity improved. However, because of the reduced blowing rate the momentum deficit associated with the boundary layer upstream of the blowing slots is compensated less effectively. Therefore, the resulting wake is less uniform than for a configuration with the blowing slots positioned more upstream.

In terms of the sensitivity of the wake uniformity to the blowing coefficient, Fig. 11 confirms the observations drawn before based on Fig. 10. The wake uniformity initially improves with increasing blowing coefficient, until an optimum is reached after which the uniformity decreases again upon further increasing the blowing rate. The change in value of the W-criterion around the optimum is relatively steep, highlighting the sensitivity of the wake uniformity to the blowing coefficient. To provide more insight into the behavior of the pylon wake with varying blowing coefficient C_μ, the wake velocity profiles at $x/c = 1.25$ are considered in Fig. 12 for a range of blowing rates.

The velocity profiles depicted in Fig. 12 once more confirm the reduction of the velocity deficit achieved by blowing. At the optimal blowing coefficient, the velocity throughout the entire pylon wake is within 1.5% of the local velocity outside of the wake. The stronger blowing jet at the highest value of C_μ resulted in a velocity overshoot around the wake centerline, hence decreasing the wake uniformity.

The shape of the velocity profile at the optimal blowing momentum coefficient corresponds to the type-B profile shown in Fig. 3. Figure 13 plots the corresponding boundary-layer profiles along vertical lines normal to the airfoil at three different chordwise positions. For comparison reasons, the results obtained at the blowing coefficients directly above and below the optimal value are also included.

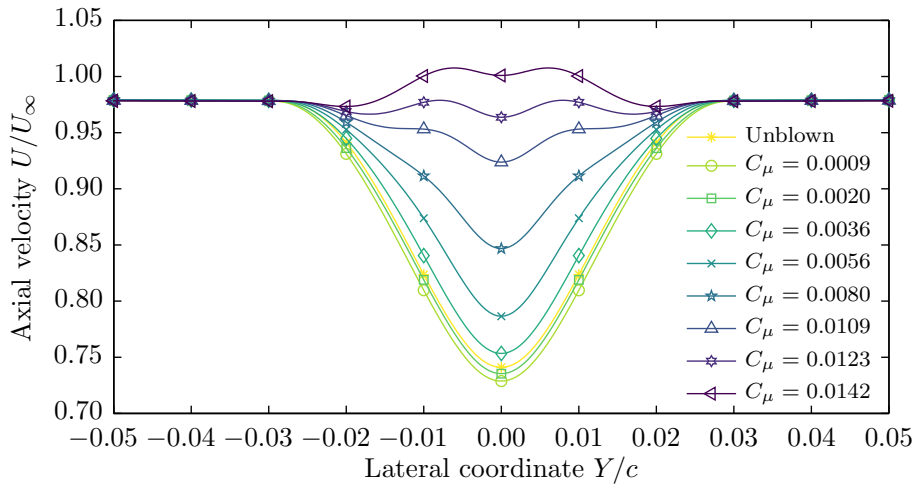

Figure 12. Velocity profiles in the blown pylon wake; $x/c = 1.25$, $x_{\text{slot}}/c = 0.7$, $h_{\text{slot}}/c = 1.0 \cdot 10^{-3}$.

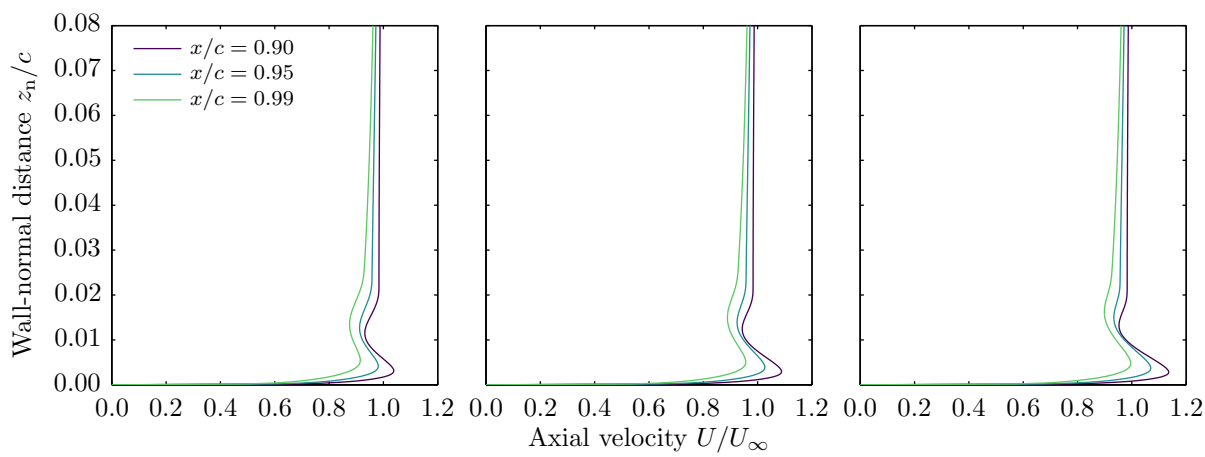

a) $C_\mu = 0.0109$ **b) $C_\mu = 0.0123$** **c) $C_\mu = 0.0142$**

Figure 13. Boundary-layer profiles; $x_{\text{slot}}/c = 0.7$, $h_{\text{slot}}/c = 1.0 \cdot 10^{-3}$.

The boundary-layer profiles given in Fig. 13 follow the generic shape shown in Fig. 2. The blowing jet accelerates the flow near the wall, leading to a local velocity overshoot. Away from the surface, the momentum deficit of the boundary layer formed upstream of the blowing slot is visible, causing a velocity deficit. The velocity deficit and overshoot should mix to end up with a uniform wake profile. This is illustrated in Fig. 14, which displays the boundary-layer profiles and resulting wake-velocity distribution at the lowest and highest blowing coefficients considered in Fig. 13. The unblown case is also included.

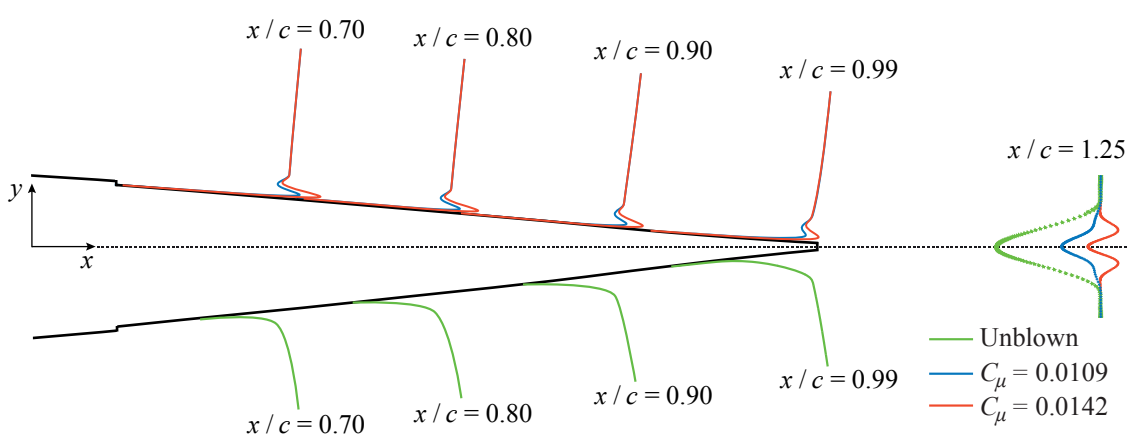

Figure 14. Typical boundary-layer development and wake velocity profiles for different blowing coefficients.

Figure 14 shows that the central minimum in the wake profile is the result of the velocity deficit caused by the development of the boundary layers downstream of the blowing slot. The two maxima, on the other hand, are the result of the extra momentum blown from the slots on both surfaces of the pylon. Finally, the two velocity minima near the wake edges are due to the remainder of the thick boundary layer that develops on the pylon surface upstream of the blowing slots. This part of the boundary layer is accelerated by the blown jets, resulting in an almost uniform wake profile at the observed transverse location downstream of the pylon trailing edge.

Comparing the boundary-layer profiles and resulting velocity distributions in the blown wake, it is clear that the uniformity of the pylon wake depends on the magnitude of the velocity overshoot in the boundary layer. A certain overshoot is required to compensate for the momentum loss in the boundary layer downstream of the blowing slot. However, if the overshoot is too large then the wake profile will be characterized by a velocity overshoot, reducing the uniformity of the propeller inflow. This confirms the conclusion that a tradeoff needs to be made between the chordwise position of the slot and the blowing momentum coefficient to achieve the most uniform velocity distribution in the pylon wake.

So far, the slot height was ignored in the process of determining the optimal blowing configuration. To illustrate its effect on the wake uniformity, Fig. 15 plots the wake velocity profiles at $x/c = 1.25$ for the three different slot heights considered in the design study. The remaining slot parameters were set to the optimal values identified before: $x_{\text{slot}}/c = 0.7$ and $C_\mu = 0.0123$. For reference, the unblown result is also shown.

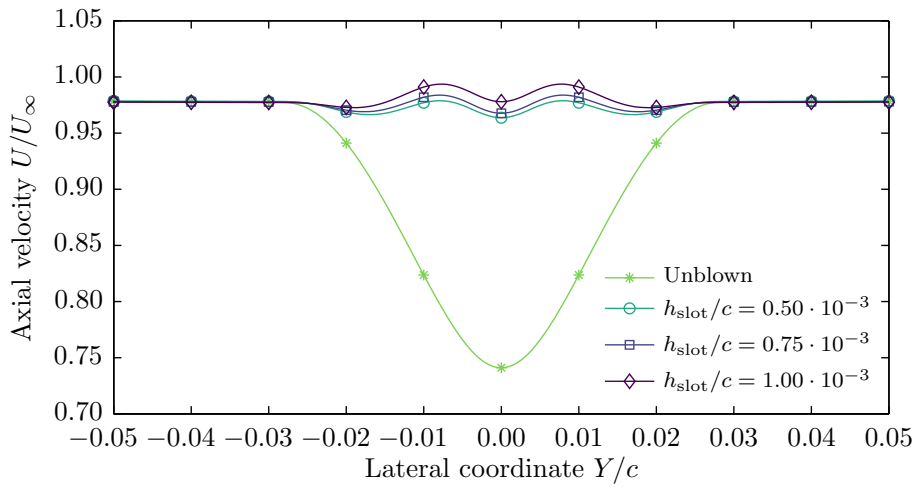

Figure 15. Effect of slot height on the wake velocity profile; $x_{\text{slot}}/c = 0.7$, $C_\mu = 0.0123$.

The velocity profiles displayed in Fig. 15 confirm that the slot height has a minor impact on the uniformity of the pylon wake. Slight differences between the velocity profiles in the wake appear because of the different shapes of the velocity profile exiting from the blowing slots. By decreasing the slot height, the velocity profile of the blown jet becomes more parabolic. This affects the mixing with the external flow, thereby modifying the velocity profile in the downstream wake. For the selected slot location and blowing coefficient, the slot height of $h_{\text{slot}}/c = 7.5 \cdot 10^{-4}$ provided the most uniform wake. Compared to the unblown case, a reduction in the W-criterion of 99.7% was achieved. A summary of the optimal slot parameters is provided in Table 7.

Table 7. Overview of selected optimal slot parameters.

Parameter	Symbol	Value
Slot position	x_{slot}/c	0.7
Slot height	h_{slot}/c	$7.5 \cdot 10^{-4}$
Blowing coefficient	C_μ	0.0123

The goal of positioning the blowing slots along the pylon chord is to increase the uniformity of the blown wake with respect to a trailing-edge blowing layout. Figure 16 compares the performance of the two types of blowing system in terms of the W-criterion versus blowing coefficient. The geometry of the chordwise blowing system featured the optimal slot position listed in Table 7 and a slot height of $h_{\text{slot}}/c = 0.001$, while the trailing-edge blowing system was the same as for the validation study discussed in Paragraph III.C.1.

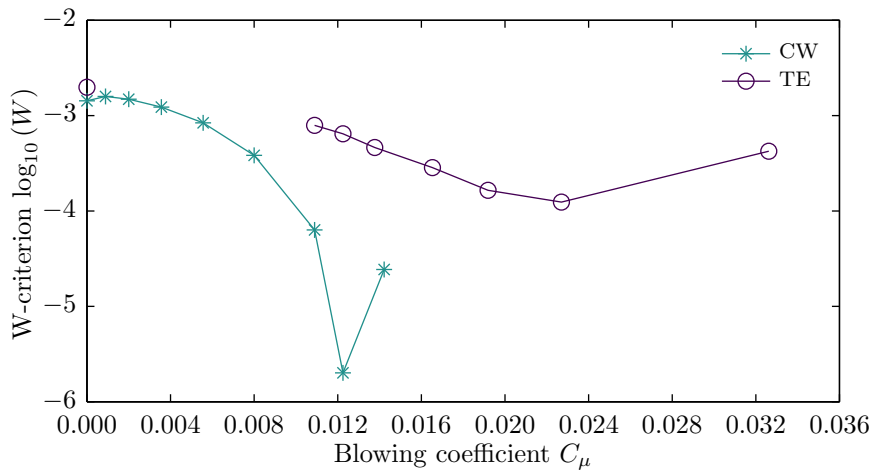

Figure 16. Wake uniformity using chordwise (CW) and trailing-edge (TE) blowing approaches; $x/c = 1.25$.

Figure 16 confirms the superior performance of the chordwise blowing layout. Using the chordwise blowing system, a much lower value of the W-criterion is reached than with the trailing-edge blowing system. Moreover, the mass flow required to reach this uniformity is lower for the chordwise blowing case. For the respective optimal values of the blowing coefficients, the total mass flow required for the trailing-edge blowing system is about 15 times higher than for the chordwise blowing system.

To further compare the wake profiles obtained with chordwise and trailing-edge blowing, Fig. 17 plots the resulting velocity distributions in the wake at $x/c = 1.25$. These results were obtained at the blowing coefficients leading to the most uniform wake for the chordwise blowing and trailing-edge blowing cases.

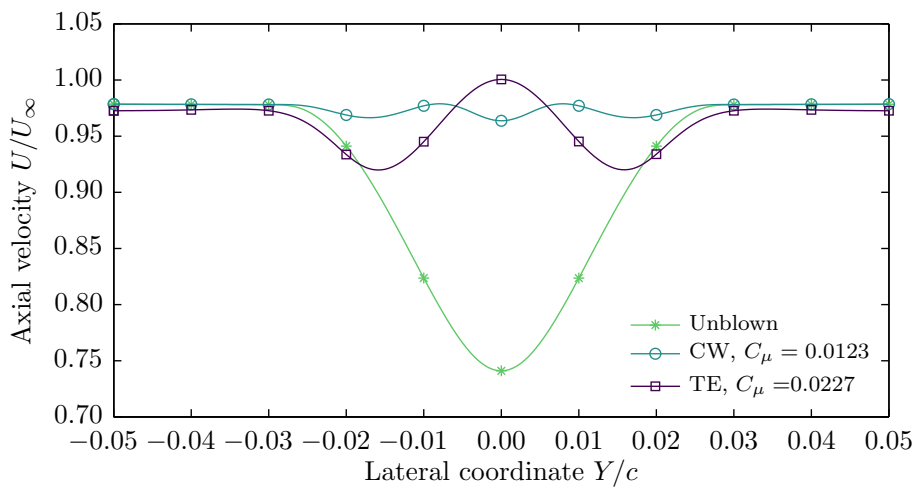

Figure 17. Optimal velocity profiles obtained using chordwise and trailing-edge blowing approaches; $x/c = 1.25$.

The velocity profiles shown in Fig. 17 illustrate the cause of the comparatively low uniformity in the pylon wake with trailing-edge blowing. The boundary layer at the pylon trailing edge is much thicker than upstream of the chordwise blowing slot. Therefore, the wake thickness is larger with trailing-edge blowing than for the chordwise blowing case. Moreover, for the trailing-edge blowing configuration the available mixing length is strongly reduced when compared to the chordwise blowing layout. Consequently, the velocity overshoot in the wake due to the high-momentum blowing jets is much more pronounced for trailing-edge blowing. Also, the deficit due to the pylon boundary layer is filled less effectively, resulting in a type-C velocity profile (Fig. 3) with relatively strong velocity fluctuations remaining for the trailing-edge blowing case.

B. Blowing Performance in Asymmetric Inflow Conditions

In case of operation in asymmetric inflow, the wake filling becomes more challenging. The effectiveness of trailing-edge blowing is reduced significantly because of the difference in boundary-layer characteristics on both sides of the pylon and the asymmetry of the resulting wake. With chordwise blowing, on the other

hand, the blowing coefficient can be optimized on each surface individually. Moreover, since the mixing between high- and low-momentum flows already starts at the pylon surface, the asymmetry of the wake no longer presents a problem for optimal wake filling.

The chordwise blowing system defined in Section IV.A was used to study the wake-filling potential at nonzero angle of attack. The blowing coefficient required in asymmetric inflow was determined from the data obtained for the symmetric case. It was shown before in Fig. 14 that the wake uniformity is dependent on the velocity overshoot and deficit in the boundary-layer profile leaving the pylon surface. The boundary-layer characteristics in turn depend on the combination of slot location and blowing coefficient. Therefore, for a fixed slot location, the blowing coefficient can be controlled to arrive at an optimally filled wake. To find the blowing coefficients required when operating at angle of attack, it is assumed here that a linear relation exists between the optimal blowing coefficient and the boundary-layer thickness at the slot location $\delta_{x_{\text{slot}}}$:

$$C_\mu^* = \lambda \delta_{x_{\text{slot}}}, \tag{5}$$

with λ a sensitivity parameter. Based on the simulations performed for the symmetric case, the value of λ was found to equal 0.97 for the configuration studied in this paper.

To successfully apply Eq. (5), first the boundary-layer thickness at the location of the blowing slot needed to be found. These were obtained from simulations of the unblown configuration at the desired angle of attack. Subsequently, Eq. (5) was used to determine the required blowing rates on both surfaces. The corresponding results are given in Table 8 for angles of attack of 3, 6, 9, and 12 degrees. For reference, the data for the symmetric inflow case are also included.

Table 8. Boundary-layer thickness and required blowing rate versus angle of attack for upper (u) and lower (l) surfaces.

α	δ_{u}	δ_{l}	$\left(C_\mu^{\text{u}}\right)^*$	$\left(C_\mu^{\text{l}}\right)^*$
0°	0.0127	0.0127	0.0123	0.0123
3°	0.0133	0.0117	0.0128	0.0113
6°	0.0156	0.0104	0.0151	0.0100
9°	0.0171	0.0099	0.0165	0.0096
12°	0.0191	0.0093	0.0184	0.0090

The blowing coefficients provided in Table 8 were used to simulate the flowfield around the blown pylons at angle of attack. Figure 18 compares the optimal velocity profiles at $x/c = 1.25$ for the cases at $\alpha = 0°$ and $\alpha = 9°$.

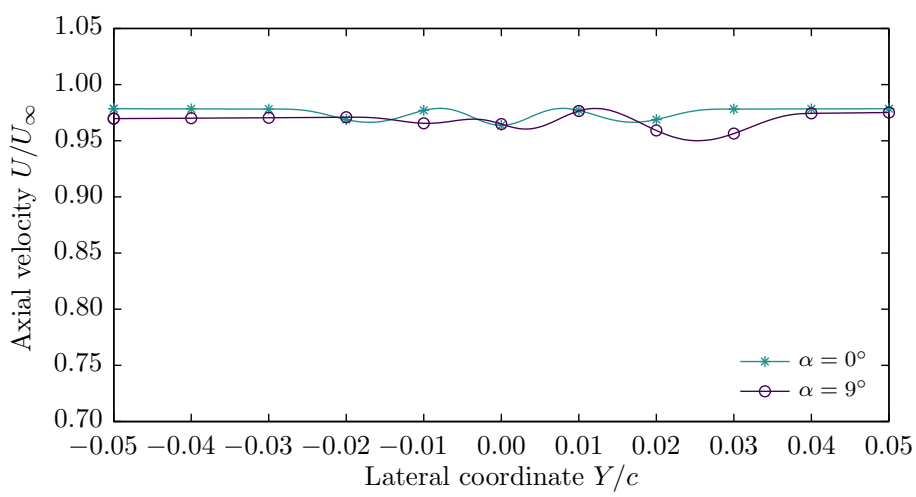

Figure 18. Effect of angle of attack on the optimal wake velocity profiles; $x/c = 1.25$.

Figure 18 confirms that, even under asymmetric flow conditions, chordwise blowing still leads to significant filling of the downstream wake. Compared to the unblown case at the same angle of attack, a reduction of the W-criterion of 99% was achieved at $\alpha = 9°$. When operated at an angle of attack, the two minima

around the central deficit in the wake velocity profile are no longer symmetric. This is because the thicker boundary layer on the upper surface of the pylon requires a longer mixing length for optimal wake filling than the thinner boundary layer on the lower surface. Since the slot locations were kept fixed at a constant chordwise position, it was not possible to fully eliminate this asymmetry in the resulting velocity profiles in the wake. Therefore, the uniformity of the blown wakes decreased slowly with increasing angle of attack.

The successful wake filling illustrated in Fig. 18 confirms the applicability of Eq. (5). Despite the complex flow physics involved, the use of a linear relation between required blowing coefficient and boundary-layer height resulted in effective wake filling at angle of attack. Further improvements of the wake uniformity in asymmetric inflow could be achieved by taking the values obtained from the simplified relation of Eq. (5) as a starting point of a more in-depth optimization study.

V. Conclusions

A numerical analysis was performed of a chordwise pylon-blowing system, targeted at minimizing the nonuniformity of the downstream wake. Such a blowing system is relevant for pusher-propeller configurations, for which the propellers operate in the wake of the upstream support pylon.

It was concluded that the optimal chordwise location of the blowing slot is determined by a compromise between boundary-layer thickness at the blowing slot, boundary-layer development downstream of the blowing slot, and available mixing length from the blowing slot to the wake-evaluation plane. For the considered configuration, a chordwise slot location around $x/c = 0.7$ was found to be optimal. The blowing coefficient should be selected such that a velocity overshoot occurs in the boundary layer directly downstream of the blowing slot. In this way, the low-momentum flow associated with the boundary layer downstream of the blowing slot can be compensated by mixing, resulting in the most uniform wake possible. With the optimal slot location and momentum coefficient defined, the impact of the slot height was concluded to be small. Using the optimal slot parameters, the chordwise blowing system provided almost full elimination of the wake, with a reduction in nonuniformity of 99.7% compared to the unblown case.

For comparison reasons, also the trailing-edge blowing case was evaluated. The optimal wake uniformity achieved with trailing-edge blowing was worse than that obtained using chordwise blowing, and required a higher blowing rate. This was the result of both the thicker boundary layer at the location of the blowing slot at the trailing edge and the reduced mixing length from blowing slot to evaluation plane in the downstream wake.

When operated at angle of attack, the boundary layer develops differently on the upper and lower surfaces of the pylon. As a result, different blowing rates are required from the two blowing slots to achieve a uniform blown wake. An empirical relation was defined between the blowing coefficient for optimal wake filling and the boundary-layer thickness at the blowing slot, based on the data obtained for the case with symmetric inflow. This relation was successfully applied to find the required asymmetric blowing rates for cases operated at angle of attack. This is relevant for realistic flight scenarios, in which the pylon–propeller combination might operate at an angle of incidence to the incoming flow.

Acknowledgments

The authors would like to thank the German Aerospace Center and in particular Dr.-Ing. Jochen Wild for providing the experimental data set that was used as validation case for the chordwise blowing layout.

References

[1]Page, M. A., Ivey, D. M., and Welge, H. R., "Ultra High Bypass Engine Applications to Commercial and Military Aircraft," *SAE Technical Paper 861720*, 1986.

[2]Block, P. J. W. and Gentry, Jr., G. L., "Directivity and Trends of Noise Generated by a Propeller in a Wake," 1986, NASA-TP-2609.

[3]Sinnige, T., Ragni, D., Malgoezar, A. M. N., Eitelberg, G., and Veldhuis, L. L. M., "APIAN-INF: an Aerodynamic and Aeroacoustic Investigation of Pylon-Interaction Effects for Pusher Propellers," *CEAS Aeronautical Journal*, 2017, advance online publication. doi: 10.1007/s13272-017-0247-2.

[4]Shivashankara, B. N., Johnson, D. P., and Cuthbertson, R. D., "Installation Effects on Counter Rotating Propeller Noise," *13th AIAA Aeroacoustics Conference*, 1990, Tallahassee, FL, USA.

[5]Ricouard, J., Julliard, E., Omaïs, M., Regnier, V., Parry, A. B., and Baralon, S., "Installation effects on contra-rotating open rotor noise," *16th AIAA/CEAS Aeroacoustics Conference*, 2010, Stockholm, Sweden.

[6]Paquet, C., Julliard, E., Genoulaz, N., Ricouard, J., and Spiegel, P., "Z08: low-speed aero-acoustic experimental characterization of open rotor installation on aircraft," *20th AIAA/CEAS Aeroacoustics Conference*, 2014, Atlanta, GA, USA.

[7]Stürmer, A., Yin, J., and Akkermans, R., "Progress in aerodynamic and aeroacoustic integration of CROR propulsion systems," *The Aeronautical Journal*, Vol. 118, No. 1208, 2014, pp. 1137–1158.

[8]Fernando, R. and Leroux, M., "Open-Rotor low speed aero-acoustics: wind tunnel characterization of an advanced blade design in isolated and installed configurations," *20th AIAA/CEAS Aeroacoustics Conference*, 2014, Atlanta, GA, USA.

[9]Sinnige, T., Ragni, D., Eitelberg, G., and Veldhuis, L. L. M., "Mitigation of Pusher-Propeller Installation Effects by Pylon Trailing-Edge Blowing," *Journal of Aircraft*, Vol. 54, No. 1, 2017, pp. 292–300.

[10]Stürmer, A. and Yin, J., "Pylon Trailing Edge Blowing for the Control of CROR Unsteady Blade Loads," *New Results in Numerical and Experimental Fluid Mechanics VIII*, edited by A. Dillmann, G. Heller, H.-P. Kreplin, W. Nitsche, and I. Peltzer, Vol. 121 of *Notes on Numerical Fluid Mechanics and Multidisciplinary Design*, Springer Berlin Heidelberg, 2013, pp. 715–722.

[11]Ben Nasr, N., Rodriguez, B., Chelius, A., and Canard-Caruana, S., "Blowing Strategies of Pylon-Propeller Configuration for Noise Reduction using Numerical Approach," *6th AIAA Flow Control Conference*, 2012, New Orleans, LA, USA.

[12]Bury, Y., Bordron, A., Belloc, H., and Prat, D., "CROR-Powerplant pylon wake mitigation for noise reduction through innovative blowing/suction-based active flow control system," *34th AIAA Applied Aerodynamics Conference*, 2016, Washington, D.C., USA.

[13]Nakayama, A., "Characteristics of the flow around conventional and supercritical airfoils," *Journal of Fluid Mechanics*, Vol. 160, 1985, pp. 155–179.

[14]Richardson, L. F., "The Approximate Arithmetical Solution by Finite Differences of Physical Problems Involving Differential Equations, With an Application to the Stresses in a Masonary Dam," *Philosophical Transactions of the Royal Society A*, Vol. 210, 1910, pp. 307–357.

[15]Richardson, L. F. and Gaunt, J. A., "The Deferred Approach to the Limit," *Philosophical Transactions of the Royal Society A*, Vol. 226, 1927, pp. 299–361.

[16]Roache, P. J., "A Method for Uniform Reporting of Grid Refinement Studies," *Symposium on Quantification of Uncertainty in Computational Fluid Dynamics*, edited by I. Celik, C. J. Chen, P. J. Roache, and G. Scheurer, Vol. 158 of *FED-ASME*, New York: American Society of Mechanical Engineers, 1993, pp. 109–120.

[17]Roache, P. J., "Perspective: A Method for Uniform Reporting of Grid Refinement Studies," *ASME Journal of Fluids Engineering*, Vol. 116, No. 3, 1994, pp. 405–413.

[18]Pfingsten, K. C. and Radespiel, R., "Experimental and numerical investigation of a circulation control airfoil," *47th AIAA Aerospace Sciences Meeting*, 2009, Orlando, FL, USA.

[19]Wild, J., "Mach and Reynolds Number Dependencies of the Stall Behavior of High-Lift Wing-Sections," *Journal of Aircraft*, Vol. 50, No. 4, 2013, pp. 1202–1216.

[20]Wild, J., "Mach-, Reynolds- and Sweep Effects on Active Flow Separation Control Effectivity on a 2-Element Airfoil Wing," *Active Flow and Combustion Control 2014*, edited by R. King, Vol. 127 of *Notes on Numerical Fluid Mechanics and Multidisciplinary Design*, Springer, Cham, 2015, pp. 87–100.